Elsevier Editorial System(tm) for Toxicon
Manuscript Draft

Manuscript Number: TOXCON-D-14-00302R1

Title: Involvement of loops 2 and 3 of α-sarcin on its ribotoxic activity

Article Type: Research Paper

Keywords: ribotoxin, cation-π interaction, SRL, Lys-rich region

Corresponding Author: Dr. Alvaro Martinez-Del-Pozo,

Corresponding Author's Institution:

First Author: Carlos Castaño-Rodríguez

Order of Authors: Carlos Castaño-Rodríguez; Miriam Olombrada; Angélica Partida-Hanon; Javier Lacadena; Mercedes Oñaderra; José G Gavilanes; Lucía García-Ortega; Alvaro Martinez-Del-Pozo

Abstract: Ribotoxins are a family of fungal ribosome-inactivating proteins displaying highly specific ribonucleolytic activity against the sarcin/ricin loop (SRL) of the larger rRNA, with α-sarcin as its best-characterized member. Their toxicity arises from the combination of this activity and their ability to cross cell membranes. The involvement of α-sarcin's loops 2 and 3 in SRL and ribosomal proteins recognition, as well as in the ribotoxin-lipid interactions involving cell penetration, has been suggested some time ago. Different mutants have been prepared in order to study the role of these loops in their ribonucleolytic and lipid-interacting properties. The results obtained confirm that loop 3 residues Lys 111, 112, and 114 are key actors of the specific recognition of the SRL. In addition, it is also shown that Lys 114 and Tyr 48 residues conform a network of interactions which is essential for the catalysis. Lipid-interaction studies show that this Lys-rich region is indeed involved in the phospholipids recognition needed to cross cell membranes. Finally, loop 2 is shown to be responsible for the conformational change which exposes the region establishing the hydrophobic interactions with the membrane inner leaflets and eases penetration of ribotoxins target cells.

Suggested Reviewers:

Opposed Reviewers:

Highlights

The role of loops 2 and 3 in the toxic activity of ribotoxins has been only poorly studied.

Results presented now confirm the key role of loop 3 Lys-111, 112, and 114 for the SRL specific recognition.

They also show the existence of a network of interactions involving Lys-114 and Tyr-48 which is essential for catalysis.

Charge reversal reveals that loop 3 Lys-rich region is involved in electrostatic interactions needed by ribotoxins to cross cell membranes.

Loop 2 loop is responsible for the conformational change needed to establish hydrophobic interactions with the membrane inner leaflets.

Introduction

Ribotoxins are a family of fungal ribosome-inactivating proteins displaying insecticidal activity (Herrero-Galán et al. 2013; Herrero-Galán et al. 2008; Olombrada et al. 2013; Olombrada et al. 2014a),with α-sarcin as its best-characterized member (Lacadena et al. 2007). They show a highly specific ribonucleolytic activity against a single phosphodiester bond of the larger rRNA, located at a universally conserved sequence motif known as the sarcin/ricin loop (SRL) (Chan et al. 1983; Endo et al. 1983).Their toxicity arises not only from this exquisite RNase specificity but also from their ability to cross cell membranes. Once inside the cell, they inactivate any known ribosome given the universal conservation of the SRL (Lacadena et al. 2007).

Most known ribotoxins show a high degree of sequence identity, above 85%. The only exception is hirsutellin A (HtA), which is produced and secreted by the invertebrate fungal pathogen *Hirsutella thompsonii* (Mazet and Vey 1995). This protein stands out because of its significantly smaller size and much lower sequence identity (only 25%; Fig. 1). However, HtA still maintains the characteristic elements of regular secondary structure as well as the nature and geometrical arrangement of most of the residues making the active site (Herrero-Galán et al. 2008; Viegas et al. 2009). On the other hand, HtA displays important differences regarding its non-structured loops. These differences are especially remarkable for the NH_2-terminal β-hairpin and loops 2 and 3 (Fig. 1). Even though, HtA maintains all functional properties of ribotoxins except for a slightly different behavior in assays with phospholipid model vesicles (Herrero-Galán et al. 2008; Yang et al. 2001).

The importance of the long loop 2 (Fig. 1; green loop) in ribotoxins functionality was suggested long time ago. It was proposed to be involved in the recognition of the SRL (Yang et al. 2001) and several ribosomal proteins (García-Mayoral et al. 2005), as well as in the ribotoxin-lipid interactions involving cell penetration (Kao and Davies 1999; Martínez-del-Pozo et al. 1988; Pérez-Cañadillas et al. 2000; Yang and Moffat 1996). In α-sarcin, the conformation of this region is stabilized in part by a conserved specific hydrogen bond between Asn54 and Ile69 (Hebert et al. 1998; Pérez-Cañadillas et al.

2002; Siemer et al. 2004), something that is not necessary in HtA because loop 2 is much shorter (Fig. 1). It was proposed that α-sarcin interacts with eukaryotic ribosomal protein L9 through the highly basic part of this loop 2, containing Lys residues 61, 64,70, 73, 81, 84, and 89 (García-Mayoral et al. 2005), a sequence stretch suggested to be also involved in membrane interactions. Interestingly, the HtA shorter loop 2 lacks this important lysine-rich surface. Finally, from structural and functional points of view, the long loop 2 of α-sarcin can be divided into two different segments due to the presence of a disulfide bridge established between Cys 76 and 132. This second segment stretch of loop 2 (residues 77 to 93) not only contains three of the mentioned Lys residues but also His 82 (Fig. 1), a residue that establishes a well defined cation-π interaction with Trp 51 (De Antonio et al. 2000; Pérez-Cañadillas et al. 1998; Pérez-Cañadillas et al. 2000). This observation is interesting considering that the protein region containing Trp51 seems to be involved in α-sarcin membrane interactions (De Antonio et al. 2000).

From the point of view of the recognition of their RNA substrate, the most significant features of the SRL structure are a GAGA tetraloop, containing the phosphodiester bond to be cleaved, and a bulged G motif (Correll et al. 1998; Correll et al. 1999). Loop 3 of α-sarcin contains three Lys residues (Lys111, Lys112 and Lys114) (Fig. 1; light blue loop) which seem to be of special importance as they appear to contact this identity bulged-G element of the ribosomal SRL region (Kao and Davies 1999; Kao and Davies 2000; Korennykh et al. 2007; Korennykh et al. 2006; Pérez-Cañadillas et al. 2000; Plantinga et al. 2008; Plantinga et al. 2011; Yang et al. 2001; Yang and Moffat 1996). Furthermore, the electrostatic interactions involving these three Lys residues of loop 3 seem to be a major contributing factor for positioning the SRL-like oligo substrate for site-specific cleavage (Plantinga et al. 2008; Plantinga et al. 2011). Interestingly, only two of these Lys residues appear to be conserved in HtA (Lys 83 and 88) (Fig. 1).

In the work herein presented, different mutant versions of α-sarcin have been produced, isolated and characterized. First, a chimeric version of α-sarcin (ΔSarHtA) has been constructed by replacing the α-sarcin stretch comprising residues 79 to 93 (second segment of loop 2) (Figure 1; gray loop) by the equivalent and much shorter HtA segment: Ala60-Asp61-Ala62-Ile63 (Fig. 1B, underlined sequences). Second, another mutant has been made in this loop 2 by replacing His82 by a Gln residue (H82Q). Finally, the three singular Lys residues of loop 3 have been also individually mutated to Glu (K111E, K112E, and K114E); involving a charge reversion. The results obtained are discussed in terms of the individual roles of these regions in α-sarcin interactions with ribosomes and biological membranes.

Materials and methods

Mutant cDNA construction

All materials and reagents were of molecular biology grade. Cloning procedures, PCR-based oligonucleotide site-directed mutagenesis, and bacterial manipulations were carried out as previously described (Álvarez-García et al. 2006; Lacadena et al. 1994; Martínez-Ruiz et al. 2001). Mutagenesis constructions were performed using different sets of complementary mutagenic primers (Table S1). Mutations were confirmed by DNA sequencing at the corresponding Complutense University facility. The plasmid used as template for mutagenesis, containing the cDNA sequence of wild-type α-sarcin, has already been described (Lacadena et al. 1994; Lacadena et al. 1999).

Protein production and purification

E. coli BL21 (DE3) cells, previously cotransformed with a thioredoxin-producing plasmid (pT-Trx) and the corresponding α-sarcin wild-type or mutant plasmids were used to produce and purify all proteins, as previously described (García-Ortega et al. 2000; Lacadena et al. 1995; Lacadena et al. 1994; Lacadena et al. 1999; Siemer et al. 2004). Fungal natural wild-type α-sarcin was produced and isolated as reported before (Martínez-Ruiz et al. 2001). Yields were always in the order of milligram amounts per liter or original culture (Table S2). SDS-PAGE of proteins, Western blots, protein hydrolysis, and amino acid analysis were performed according to standard procedures, also as previously described (Lacadena et al. 1994; Martínez-Ruiz et al. 2001).

Spectroscopic characterization

Spectroscopic characterization was performed following well-established procedures (Álvarez-García et al. 2009a; Álvarez-García et al. 2006; García-Ortega et al. 2001; García-Ortega et al. 2005; García-Ortega et al. 2002; Lacadena et al. 1999; Martínez-Ruiz et al. 2001). Absorbance measurements were carried out on a Beckman DU640 spectrophotometer (Beckman Coulter, Brea, CA, USA) at 200 nm/min scanning speed and room temperature. Amino acid analyses and the corresponding UV-absorbance spectra were also used to calculate their extinction coefficients (Table S2). Circular dichroism spectra were obtained in a Jasco 715 spectropolarimeter (Jasco, Easton, MD, USA), equipped with a thermostated cell holder and a Neslab-111 circulating water bath, at 0.2 nm/s scanning speed. Thermal denaturation profiles were obtained by measuring the temperature dependence of the ellipticity at 220 nm in the 25–80 °C range using a rate of temperature increment of 30ºC per hour. Fluorescence emission spectra were recorded on an SLM Aminco 8000 spectrofluorimeter at 25°C using a slit width of 4 nm for both excitation and emission beams. The spectra were recorded for excitation at 275 and 295 nm and both were normalized by considering that Tyr emission above 380 nm is negligible. The Tyr contribution was calculated as the difference between the two normalized spectra. Thermostated cells with a path length of 0.2 and 1.0 cm for the excitation and emission beams, respectively, were used. All these experiments were performed in 50 mM sodium phosphate, pH 7.0, containing 0.1 M NaCl.

Ribonucleolytic activity assays

The ribonucleolytic activity of α-sarcin on rabbit ribosomes was followed by detecting the release of the specific 400-nt α-fragment from the ribosomes of a cell-free rabbit reticulocyte lysate (Promega) as described (Kao et al. 2001). Visualization of this α-fragment was performed by ethidium bromide staining of 2.4% agarose gels after electrophoretic fractionation of the samples using denaturing conditions.

The specific cleavage by ribotoxins of a 35-mer synthetic oligonucleotide mimicking the sequence and structure of the SRL was also analyzed as described before (Kao et al. 2001). The sequence of this oligo was 5’-

GGGAAUCCUGCUCAGUACGAGAGGAACCGCAGGUU-3’, where the cleavage site by α-sarcin appears underlined. Synthesis of this SRL-like RNA oligo was performed as previously described (García-Ortega et al. 2010; Kao et al. 2001). Reaction products were run on a denaturing 19 % (w/v) polyacrylamide gel and visualized by ethidium bromide staining.

The absence of contaminating non-specific RNase-like activities in the protein preparations employed was ruled out in all protein batches employed by means of zymogram assays against poly(A) (Kao et al. 2001; Lacadena et al. 1995; Lacadena et al. 1994; Lacadena et al. 1999). These assays were also used to evaluate the non-specific residual ribonucleolytic activity of the proteins studied against non-structured substrates.

Phospholipid vesicle assays

DMPG (1,2-dimyristoyl-sn-glycero-3-phosphoglycerol) was purchased from Avanti Polar Lipids Inc. (Alabaster, Alabama, U.S.A.). Vesicles were formed in 15 mM Tris-HCl, pH 7.0, containing 0.1M NaCl and 1 mM EDTA, as previously described (Mancheño et al. 1994; Martínez-Ruiz et al. 2001). Phospholipid concentration was also determined as described (Bartlett 1959). Analysis of protein binding to vesicles was performed by ultracentrifugation (Alegre-Cebollada et al. 2006; Martínez-Ruiz et al. 2001) using samples prepared at different lipid to protein molar ratios which were incubated at 37ºC for 1 h and then centrifuged at 164000 g for 1 h at 4ºC in a 42.2 Ti Beckman rotor. The amount of protein that did not sediment with the vesicles was determined from the absorbance spectra of the supernatant, and the concentration of ribotoxin bound to the liposomes was then calculated taking into account the initial concentration of protein (10 μM in all cases). Aggregation was monitored as described before (Gasset et al. 1989) by measuring the increase of the absorbance at360 nm of a suspension of vesicles (30 μM final lipid concentration) after addition of a small aliquot of a freshly prepared solution of protein. Leakage of vesicle aqueous contents was measured by using the 8-aminonaphthalene-1,3,6-trisulfonic acid/N,N-p-xilene-bispyridiniumbromide (ANTS/DPX) assay as previously described (Mancheño et al. 1998). Other experimental details were as previously reported (Gasset et al. 1994; Gasset et al. 1995; Gasset et al. 1991a; Gasset et al. 1991b; Gasset et al. 1990; Mancheño et al. 1995; Mancheño et al. 1994; Oñaderra et al. 1993).

Insect cells culture and toxicity assays

The insect cell line *S. frugiperda* (Sf9) was cultured as described (Olombrada et al. 2013; Tello et al. 2010) in Insect-XPRESS^{TM} Protein-free Insect Cell medium (BioWhittaker) at 27 ºC as indicated by the manufacturer. Protein solutions were prepared in Insect X-press medium and sterilized by ultrafiltration. Protein biosynthesis inhibition assays were made seeding Sf9 cells into 24-well plates at a cell density of 10^5 cells/well and were maintained under standard culture conditions up to 80% confluency (2 days). Then, monolayer cultures were incubated in 0.5 mL of fresh medium with serial dilutions of ribotoxin from 5.0 mM to 0.5 nM final concentrations. Following 18 h of incubation at 27 ºC the medium was replaced by culture medium supplemented with 0.5 µCi/well of [^{3}H]-leucine. After 5 h of incubation the medium was removed and cell protein content was precipitated with 5% trichloroacetic acid (TCA) and washed three times with ethanol. The precipitate was dried, dissolved in 200 mL of 0.1 N NaOH, 0.1% SDS and radioactivity was measured in a Beckman LS 3801 liquid scintillation counter. Results are expressed as percentage of incorporated radioactivity relative to samples without protein added.

Results

Protein purification and spectroscopic characterization

Wild-type α-sarcin and the five different mutants produced were purified to homogeneity according to their SDS–PAGE behavior (Fig. S1).Their amino acid composition was consistent with the mutation expected. All of them were also detected by a rabbit anti-α-sarcin serum in Western blot assays (Fig. S1).

Far and near-UV CD spectra of α-sarcin K111E, K112E, and K114E were practically indistinguishable from those ones corresponding to the wild-type protein (Fig. 2 and 3). Only the K114E mutant showed minor changes in the near-UV region. The far and near-UV circular dichroism spectra of ΔSarHtA were different from that corresponding to the wild-type protein (Figs. 2 and 4), but they still corresponded to a structured polypeptide. In fact, the near-UV spectrum revealed the presence of tertiary structure in the mutant variant in spite of the spectral changes observed. The calculated difference spectra wild-type *minus* mutant (Fig.2) clearly resemble those corresponding to Trp-51 deduced for the W51F mutant variant of the protein (De Antonio et al. 2000). Finally, the α-sarcin H82Q mutant also showed significant variation in both UV wavelengths regions studied (Fig. 2 and 4). These last two spectra were almost coincident to those obtained before for the W51F mutant of the same protein (De Antonio et al. 2000), confirming the already proposed interaction between the side-chains of Trp51 and His82 (De Antonio et al. 2000; Pérez-Cañadillas et al. 1998; Pérez-Cañadillas et al. 2000).

In accordance with the near-UV CD spectra, the three K111E, K112E, and K114E mutants also showed very similar fluorescence emission spectra when compared to the wild-type protein (Table S2, spectra not shown). Fluorescence emission spectra for both ΔSarHtA and H82Q mutants (Fig. 5) showed a remarkable enhancement of their Trp quantum yields (Table S2) and a slight red-shift of about 5 nm. In both cases, this observation is again in agreement with the loss of the His82-Trp51 interaction (De Antonio et al. 2000).

Ribonucleolytic characterization

Ribotoxins are highly specific RNases against ribosomes. They still retain this specificity when assayed against naked RNA containing the SRL sequence and structure. This is why its ribonucleolytic activity can be studied using a 35mer SRL-like oligomer which lacks any other additional ribosomal structural feature. However, they can also cause extensive, non-specific, progressive digestion of RNA when used at higher concentrations (Endo et al. 1988; Wool 1996; Wool 1997), including homopolynucleotides (Kao et al. 2001). The loss of specificity of these assays is compensated by the possibility of obtaining useful information about catalysis *per se*, independently of the degree of specific binding of the protein analyzed. Thus, although they are less specific, these assays have contributed significantly to the detailed study of the cleavage mechanism of ribotoxins (Álvarez-García et al. 2009b; García-Ortega et al. 2002; Kao et al. 2001; Lacadena et al. 1995; Lacadena et al. 1999; Martínez-Ruiz et al. 2001).

The three K111E, K112E, and K114E mutants, as well as the ΔSarHtA variant, were unable to achieve the ribotoxins specific ribonucleolytic cleavage of the ribosomal SRL when assayed in standard conditions against intact ribosomes in a cell-free reticulocyte lysate (Fig. 6A) even at high enzyme concentration (range assayed: 60-200 nM). The α-sarcin H82Q mutant retained about 80% of the wild-type protein ribonucleolytic activity (Fig. 6A). Nearly identical results were also obtained when using a 35-mer SRL-like oligoribonucleotide (Fig. 6B), a less specific substrate. Finally, the ribonucleolytic activity was tested using zymogram assays performed in polyacrylamide gels containing the non-specific substrate homopolynucleotide poly(A) (Fig. 6C). In this case, only the ΔSarHtA mutant did not show detectable activity, while the K111E, K112E and H82Q mutants were as active as the wild-type. Interestingly, the α-sarcin K114E variant was still much less active (Fig. 6C). These zymogram experiments were also employed to discard the presence of trace amounts of non-specific ribonucleolytic contaminants in the samples used.

Overall, this ribonucleolytic characterization suggested that ΔSarHtA had lost completely its ability to behave as an RNase while the three Lys to Glu mutants were devoid of the distinctive and unique specificity of ribotoxins but still maintained non-specific activity against single stranded non-structured RNA stretches. α-Sarcin H82Q still showed a very similar ribonucleolytic behavior as the wild-type protein.

Interaction with phospholipid vesicles

All protein variants studied bound to DMPG vesicles showing very similar behavior and stoichiometry as the wild-type α-sarcin (Fig. 7A). Only K111E and K114E showed a slightly diminished binding affinity in terms of the amount of protein needed to reach saturation. In accordance with this observation, these two variants were also less effective in aggregating the vesicles (Fig. 7B), suggesting that conserved Lys 111 and Lys 114 residues participate not only in SRL recognition but also in the protein-lipid interactions needed to enter the ribotoxins cellular targets. α-Sarcin mutants H82Q and ΔSarHtA showed the opposite behavior, displaying enhanced aggregation ability.

It is well known that α-sarcin interacts with lipid vesicles containing an abundance of acid phospholipids. This interaction results in vesicle aggregation, intermixing of phospholipids from different vesicles, and leakage of the aqueous contents of its target vesicles. However, HtA does not promote vesicle aggregation, but still perturbed the permeability barrier of the phospholipid bilayers as shown in leakage experiments (Herrero-Galán et al. 2008). Quantitatively, HtA had in fact a higher membrane-permeabilizing ability than α-sarcin (Herrero-Galán et al. 2008). Therefore leakage induced by the present α-sarcin mutants was also studied. As can be observed in Fig. 7C, ΔSarHtA and K111E mutants showed leakage activity almost indistinguishable from that displayed by the wild-type protein, while the other two lysine mutants, K112E and K114E, were less active. The most striking result was however obtained for α-sarcin H82Q. This mutant produced massive release of the phospholipid vesicle aqueous contents at much smaller concentrations than the other proteins, wild-type α-sarcin or HtA (Herrero-Galán et al. 2008) included. This result suggests that the substitution of His 82 by a Gln residue produces a local conformational change which most probably exposes lipid interacting residues which remain buried in the wild-type protein.

Toxicity against cultured insect cells

It has been recently shown the dramatic effect of wild-type α-sarcin on the inhibition of *in vivo S. frugiperda* cells protein biosynthesis (Olombrada et al., 2013). Therefore, this insect cellular line was chosen to evaluate the toxic effect of the mutants studied when employed against intact cells. As can be seen in Fig. 8, with the only exception of α-sarcin H82Q, all the other mutants were virtually devoid of toxic activity when evaluated in terms of the IC_{50} values needed to inhibit protein biosynthesis. Interestingly, and in good agreement with all the other results showed above, the H82Q mutant showed a toxic behavior which was indistinguishable from that shown by the wild-type ribotoxin.

Discussion

Structural characterization

The spectroscopic characterization of the different α-sarcin protein variants showed that only very minor structural modifications were introduced upon replacing Lys 111, Lys 112, or Lys 114 by a glutamic acid residue. Only K114E showed clear changes in the near-UV CD spectrum related to some aromatic amino acid (Fig. 3), suggesting that switching one positive charge by a negative one may influence the microenvironment of some aromatic residue located in the vicinity of Lys 114 side-chain. In fact, in the wild-type protein structure of α-sarcin the phenol moieties of Tyr 48 and Tyr 106 are within hydrogen bonding distances of the ε amino group of Lys 114 (Fig. 9). The other two mutated Lys residues are oriented towards the solvent (Figs. 1 and 9). Accordingly, the stability of K111E and K112E remained unaltered in terms of their T_m values (Table S2), while it decreased for K114E. Altogether, and taking into account that α-sarcin fluorescence emission spectrum is dominated by Trp 4 (De Antonio et al., 2000), this geometrical arrangement would also explain why the fluorescence emission of the three Lys to Glu variants remained practically unaffected.

The other single residue mutant variant, H82Q, showed unique spectroscopic features. Both far- and near-UV spectra changed substantially (Figs. 2 and 4) and a dramatic Trp emission enhancement was observed (Fig. 5 and Table S2). The CD changes can be easily explained considering that it has been well documented how Trp 51 is not only responsible for most of the optical anisotropy of α-sarcin in the near-UV region but also that it displays a significant contribution in the far-UV (De Antonio et al. 2000). This observation was explained by the cation-π interaction established between the Trp51 side-chain and the ring of His 82 (De Antonio et al. 2000), an interaction which would be absent in the H82Q mutant. Accordingly, the far-UV CD spectrum of this variant (Fig. 2) is practically indistinguishable from that one reported before for the W51F mutant (De Antonio et al., 2000). Regarding the fluorescence emission results of α-sarcin H82Q (Fig. 5), the positively charged His 82 imidazol ring promotes strong quenching on the indole side-chain of Trp 51, the emission of the wild-type protein arising from Trp-4 (De Antonio et al., 2000). Therefore, a large increase in the fluorescence emission of Trp-51 must be observed upon disappearance of the H82-Trp-51 interaction in the H82Q mutant variant, and would also explain why this H82Q mutant shows the lowest T_m value of all the proteins herein studied (Table S2).

A dramatic structural change was introduced in the ΔSarHtA mutant since the α-sarcin loop 2 stretch (PPKHSKDGNGKTDHY) was replaced by the sequence ADAI at the equivalent region in HtA. Nevertheless, the mutant protein is still folded, as the CD study revealed, and it seemed to retain most of the folding of the wild-type protein. The existence of a well-defined two-state thermal transition of this protein variant, with a T_m value of only four degrees lower than the natural protein (Table S2), confirmed the adoption of a globular conformation. In addition, the calculated CD spectra WT *minus* ΔSarHtA resemble the Trp51 optical anisotropy contribution (De Antonio et al. 2000). In fact, the CD and fluorescence emission properties of the ΔSarHtA protein variant, where His-82 is absent, are also strongly similar to those of H82Q.

Ribonucleolytic activity

Only the H82Q mutant retained the unique and highly specific ribonucleolytic activity against ribosomes which is the distinctive feature of fungal ribotoxins (Fig. 6A). This is in good accordance with the previously observed minor changes in the enzymatic activity of W51F α-sarcin (De Antonio et al. 2000). On the contrary, the three lysine residues mutated have been suggested to be important for the specific recognition of the SRL (Dey et al. 2007; Glück and Wool 2002; Kao and Davies 1999; Kao and Davies 2000; Korennykh et al. 2007; Korennykh et al. 2006; Pérez-Cañadillas et al. 2000; Plantinga et al. 2008; Plantinga et al. 2011; Yang et al. 2001; Yang and Moffat 1996). It has been even described that these lysine residues would contribute to the formation of the enzyme:substrate complex (when assayed against a SRL-like oligo), thereby positioning it for site-specific cleavage (Plantinga et al. 2008). An observation which agrees with the fact that the Lys 114 residue has been reported to contact the bulged-G in a sequence specific manner (Glück and Wool 2002; Yang et al. 2001). Therefore, these results of enzymatic activity would confirm the already proposed key role for these Lys residues in SRL recognition.

However, the most striking result obtained refers to the ability of α-sarcin to cleave rather non-specific substrates such as poly(A). As can be seen in Fig. 6C, replacing the solvent exposed Lys 111 and 112 residues does not affect the ability of this protein to cleave this homopolynucleotide in zymogram assays. This would also agree with the mentioned role of these residues in the specific recognition of the SRL rather than taking part in the catalysis. That is to say, they are key residues for specific binding, but not for catalysis. In fact, it has been described how replacing the mitogillin ribotoxin Lys 111 (the equivalent of α-sarcin Lys 112) by Gln produced a slightly more active mutant than the wild-type protein when assayed against poly(I) (Kao and Davies 2000). On the other hand, α-sarcin K114E is almost devoid of ribonucleolytic activity, even against the non-specific substrate (Fig. 6C). Taking into account the spatial relationship established between the ε amino group of Lys 114 and the OH of Tyr 48 (Fig. 8), and given that removal of that OH renders a completely inactive version of α-sarcin (Álvarez-García et al. 2006), this interaction would explain why the K114E mutant is also unable to cleave poly(A) and shows how these two amino acids, Lys 114 and Tyr 48, must conform a network of interactions which is essential for the catalysis exerted by this protein.

Finally, the ΔSarHtA mutant was fully inactive against the three type of substrates assayed, suggesting that the second segment of loop 2 affects the geometrical arrangement of the active site.

Interaction with phospholipid vesicles.

The SRL is a universally conserved ribosomal structure but cells are only killed if ribotoxins cross their membranes to gain access to the ribosomes. As no protein receptors have so far been reported for α-sarcin, its toxic specificity has been related to a differential interaction with the negatively charged phospholipids of the membranes (Gasset et al. 1989). Using light-scattering stopped-flow kinetics it was revealed that the initial step of the interaction of α-sarcin with phospholipid vesicles is the formation of vesicle dimers maintained by protein-protein bridges (Mancheño et al. 1994). This initial aggregation is followed by a destabilizing effect of the protein which promotes vesicles fusion. As a final step, and most probably as a consequence of the formation of large unstable lipidic structures, α-sarcin also modifies the permeability of the membranes, causing leakage of the vesicles contents (Gasset et al. 1990).

According to the accepted hypothesis to explain the innate ability of α-sarcin to translocate across a phospholipid membrane (Oñaderra et al. 1993), the protein would be initially adsorbed to the charged polar head groups of the phospholipids and then would penetrate the interface of the bilayer, establishing a hydrophobically driven interaction with the lipid hydrocarbon chains (Gasset et al. 1991a; Gasset et al. 1991b). Within this idea, the region comprising a hydrophobic stretch of 24 amino acids (residues 116–139) would be responsible for this hydrophobic component of the interaction (Mancheño et al. 1995; Mancheño et al. 1998).This sequence is contiguous to the mutated lysine residues of loop 3(Fig. 1B) and contains His 137, one of the catalytically essential residues of α-sarcin (Lacadena et al. 1995; Lacadena et al. 1999). Finally, using two different Trp mutants, it was also shown that neither Trp4 nor Trp51 were required for the interaction of α-sarcin with lipid membranes (De Antonio et al. 2000). However, this interaction promoted a large increase in the quantum yield of Trp51, the residue interacting with the indole side-chain of His 82.These results indicated that the region around Trp 51, the first β-strand of the β-sheet, is also located near the hydrophobic core of the bilayer following interaction with the vesicles.

The results presented now reveal no major differences when binding was studied by ultracentrifugation. This approach primarily accounts for the tightly bound protein fraction, most probably that one driven by the hydrophobic component. Consequently, these results could be expected given that the 116-139 sequence has not been modified in any of the mutants herein studied. If we focus on the vesicle aggregation experiments (Fig. 7B), three different types of behavior can be observed. K112E mutant behaves indistinguishable from the wild-type α-sarcin. On the contrary, K111E and K114E show a diminished aggregation ability suggesting that these two Lys residues participate in the electrostatic interactions needed to bring the vesicles into close contact, as had been suggested before (Kao and Davies 1999; Martínez-del-Pozo et al. 1988; Pérez-Cañadillas et al. 2000; Yang and Moffat 1996). This proposal would also agree with the results shown in Fig. 6C, where the mutants showing less leakage capacity also involve residues of this Lys-rich region. The other two mutants (H82Q and ΔSarHtA) slightly favored aggregation. Relaxing the protein structure by the absence of the mentioned cation-π interaction involving His-82 would result in exposure of hydrophobic areas promoting an improved membrane destabilizing activity of the polypeptide, easing the interaction with the membrane hydrophobic inner leaflets and the lysis of the vesicles.

Toxicity against intact cells

The unique and highly specific ribonucleolytic activity of ribotoxins is their trademark feature which explains their extreme toxicity once inside a cell (Endo et al., 1983; Lacadena et al., 2007; Olombrada et al., 2014b). Therefore, and given that only the H82Q mutant retained this highly specific ribonucleolytic activity against ribosomes (Fig. 6A), it is quite straightforward to explain why this mutant was also the only one retaining the α-sarcin ability to inhibit protein biosynthesis when assayed against intact cells (Fig. 8).

Conclusions

The role of α-sarcin's loop 2 in the toxic activity of this protein has been only poorly studied so far. On the other hand, the Lys-rich cluster of loop 3 is well acknowledged as a key element in the specific recognition of the SRL. The results presented now confirm these observations for loop 3 Lys111, Lys112, and Lys114 residues. In addition, they also show the existence of a previously undetected network of interactions involving Lys114 and Tyr48 residues which seems to be essential for the catalysis exerted by α-sarcin. Finally, the Lys mutants studied now involve a change from positive to negative charge which impairs the interaction with the lipid vesicles. Therefore, this charge reversal reveals that this Lys-rich region of loop 3 is involved in the electrostatic phospholipid interactions needed by ribotoxins to cross cell membranes. Regarding loop 2, it is also shown now how this loop seems to be responsible for the conformational change that exposes the region establishing the hydrophobic interactions with the membrane inner leaflets, easing penetration of ribotoxins into their target cells.

Acknowledgments

This work was supported by project BFU2012-32404 from the Spanish Ministerio de Economía y Competitividad. M.O. is recipient of a FPU predoctoral fellowship from the Spanish Ministerio de Educación. L.G.-O. is a postdoctoral researcher of the PICATA program from the Campus de Excelencia Internacional Moncloa.

References

Alegre-Cebollada, J, Rodríguez-Crespo, I, Gavilanes, JG and Martínez-del-Pozo, A (2006) Detergent-resistant membranes are platforms for actinoporin pore-forming activity on intact cells. *FEBS J* **273**: 863-871.

Álvarez-García, E, García-Ortega, L, De los Ríos, V, Gavilanes, JG and Martínez-del-Pozo, A (2009a) Influence of key residues on the heterologous extracellular production of fungal ribonuclease U2 in the yeast *Pichia pastoris*. *Protein Expr Purif* **65**: 223-229.

Álvarez-García, E, García-Ortega, L, Verdun, Y, Bruix, M, Martínez-del-Pozo, A and Gavilanes, JG (2006) Tyr-48, a conserved residue in ribotoxins, is involved in the RNA-degrading activity of α-sarcin. *Biol Chem* **387**: 535-541.

Álvarez-García, E, Martínez-del-Pozo, A and Gavilanes, JG (2009b) Role of the basic character of α-sarcin's NH_2-terminal β-hairpin in ribosome recognition and phospholipid interaction. *Arch Biochem Biophys* **481**: 37-44.

Bartlett, GR (1959) Colorimetric assay methods for free and phosphorylated glyceric acids. *J Biol Chem* **234**: 469-471.

Correll, CC, Munishkin, A, Chan, YL, Ren, Z, Wool, IG and Steitz, TA (1998) Crystal structure of the ribosomal RNA domain essential for binding elongation factors. *Proceedings of the National Academy of Sciences USA* **95**: 13436-13441.

Correll, CC, Wool, IG and Munishkin, A (1999) The two faces of the *Escherichia coli* 23 S rRNA Sarcin/Ricin domain: the structure at 1.11 A resolution. *J Mol Biol* **292**: 275-287.

Chan, YL, Endo, Y and Wool, IG (1983) The sequence of the nucleotides at the α-sarcin cleavage site in rat 28 S ribosomal ribonucleic acid. *J Biol Chem* **258**: 12768-12770.

De Antonio, C, Martínez-del-Pozo, A, Mancheño, JM, Oñaderra, M, Lacadena, J, Martínez-Ruiz, A, Pérez-Cañadillas, JM, Bruix, M and Gavilanes, JG (2000) Assignment of the contribution of the tryptophan residues to the spectroscopic and functional properties of the ribotoxin α-sarcin. *Proteins* **41**: 350-361.

DeLano, WL (2008) ThePyMOL Molecular Graphics System. *San Diego, California*.

Dey, P, Tripathi, M and Batra, JK (2007) Involvement of loops l2 and L4 of ribonucleolytic toxin restrictocin in its functional activity. *Protein Pept Lett* **14**: 125-129.

Endo, Y, Chan, Y-L, Lin, A, Tsurugi, K and Wool, I (1988) The cytotoxins α-sarcin and ricin retain their specificity when tested on a synthetic oligoribonucleotide (35-mer) that mimics a region of 28 S ribosomal ribonucleic acid. *J Biol Chem* **263**: 7917-7920.

Endo, Y, Huber, PW and Wool, IG (1983) The ribonuclease activity of the cytotoxin α-sarcin. The characteristics of the enzymatic activity of α-sarcin with ribosomes and ribonucleic acids as substrates. *J Biol Chem* **258**: 2662-2667.

García-Mayoral, F, García-Ortega, L, Álvarez-García, E, Bruix, M, Gavilanes, JG and Martínez-del-Pozo, A (2005) Modeling the highly specific ribotoxin recognition of ribosomes. *FEBS Lett* **579**: 6859-6864.

García-Ortega, L, Alvarez-Garcia, E, Gavilanes, JG, Martinez-del-Pozo, A and Joseph, S (2010) Cleavage of the sarcin-ricin loop of 23S rRNA differentially affects EF-G and EF-Tu binding. *Nucleic Acids Res* **38**: 4108-4119.

García-Ortega, L, Lacadena, J, Lacadena, V, Masip, M, de Antonio, C, Martínez-Ruiz, A and Martínez-del-Pozo, A (2000) The solubility of the ribotoxin α-sarcin, produced as a recombinant protein in *Escherichia coli*, is increased in the presence of thioredoxin. *Lett Appl Microbiol* **30**: 298-302.

García-Ortega, L, Lacadena, J, Mancheño, JM, Oñaderra, M, Kao, R, Davies, J, Olmo, N, Martínez-del-Pozo, A and Gavilanes, JG (2001) Involvement of the amino-terminal β-hairpin of the *Aspergillus* ribotoxins on the interaction with membranes and nonspecific ribonuclease activity. *Protein Sci* **10**: 1658-1668.

García-Ortega, L, Lacadena, J, Villalba, M, Rodríguez, R, Crespo, JF, Rodríguez, J, Pascual, C, Olmo, N, Oñaderra, M, Martínez-del-Pozo, A and Gavilanes, JG (2005) Production and characterization of a noncytotoxic deletion variant of the *Aspergillus fumigatus* allergen Asp f 1 displaying reduced IgE binding. *Febs J* **272**: 2536-2544.

García-Ortega, L, Masip, M, Mancheño, JM, Oñaderra, M, Lizarbe, MA, García-Mayoral, MF, Bruix, M, Martínez-del-Pozo, A and Gavilanes, JG (2002) Deletion of the NH_2-terminal β-hairpin of the ribotoxin α-sarcin produces a nontoxic but active ribonuclease. *J Biol Chem* **277**: 18632-18639.

Gasset, M, Mancheño, JM, Lacadena, J, Turnay, J, Olmo, N, Lizarbe, MA, Martínez-del-Pozo, A, Oñaderra, M and Gavilanes, JG (1994) α-Sarcin, a ribosome-inactivating protein that translocates across the membrane of phospholipid vesicles. *Curr Top Pept Protein Res* **1**: 99-104.

Gasset, M, Mancheño, JM, Laynez, J, Lacadena, J, Fernández-Ballester, G, Martínez-del-Pozo, A, Oñaderra, M and Gavilanes, JG (1995) Thermal unfolding of the cytotoxin α-sarcin: Phospholipid binding induces destabilization of the protein structure. *Biochim Biophys Acta* **1252**: 126-134.

Gasset, M, Martínez-del-Pozo, A, Oñaderra, M and Gavilanes, JG (1989) Study of the interaction between the antitumour protein α-sarcin and phospholipid vesicles. *Biochem J* **258**: 569-575.

Gasset, M, Oñaderra, M, Goormaghtigh, E and Gavilanes, JG (1991a) Acid phospholipid vesicles produce conformational changes on the antitumour protein α-sarcin. *Biochim Biophys Acta* **1080**: 51-58.

Gasset, M, Oñaderra, M, Martínez-del-Pozo, A, Schiavo, GP, Laynez, J, Usobiaga, P and Gavilanes, JG (1991b) Effect of the antitumour protein

α-sarcin on the thermotropic behavour of acid phospholipid vesicles. *Biochim Biophys Acta* **1068**: 9-16.

Gasset, M, Oñaderra, M, Thomas, PG and Gavilanes, JG (1990) Fusion of phospholipid vesicles produced by the anti-tumour protein α-sarcin. *Biochem J* **265**: 815-822.

Glück, A and Wool, IG (2002) Analysis by systematic deletion of amino acids of the action of the ribotoxin restrictocin. *Biochim Biophys Acta* **1594**: 115-126.

Hebert, EJ, Giletto, A, Sevcik, J, Urbanikova, L, Wilson, KS, Dauter, Z and Pace, CN (1998) Contribution of a conserved asparagine to the conformational stability of ribonucleases Sa, Ba, and T1. *Biochemistry* **38**: 16192-16200.

Herrero-Galán, E, García-Ortega, L, Olombrada, M, Lacadena, J, Martínez-del-Pozo, A, Gavilanes, JG and Oñaderra, M (2013) Hirsutellin A: A Paradigmatic Example of the Insecticidal Function of Fungal Ribotoxins. *Insects* **4**: 339-356.

Herrero-Galán, E, Lacadena, J, Martínez-del-Pozo, A, Boucias, DG, Olmo, N, Oñaderra, M and Gavilanes, JG (2008) The insecticidal protein hirsutellin A from the mite fungal pathogen *Hirsutella thompsonii* is a ribotoxin. *Proteins* **72**: 217-28.

Kao, R and Davies, J (1999) Molecular dissection of mitogillin reveals that the fungal ribotoxins are a family of natural genetically engineered ribonucleases. *J Biol Chem* **274**: 12576-12582.

Kao, R and Davies, J (2000) Single amino acid substitutions affecting the specificity of the fungal ribotoxin mitogillin. *FEBS Letters* **466**: 87-90.

Kao, R, Martinez-Ruiz, A, Martinez del Pozo, A, Crameri, R and Davies, J (2001) Mitogillin and related fungal ribotoxins. *Methods Enzymol* **341**: 324-335.

Korennykh, AV, Correll, CC and Piccirilli, JA (2007) Evidence for the importance of electrostatics in the function of two distinct families of ribosome inactivating toxins. *RNA **13**: 1391-1396.*

Korennykh, AV, Piccirilli, JA and Correll, CC (2006) The electrostatic character of the ribosomal surface enables extraordinarily rapid target location by ribotoxins. *Nat Struct Mol Biol* **13**:436-443.

Lacadena, J, Álvarez-García, E, Carreras-Sangrà, N, Herrero-Galán, E, Alegre-Cebollada, J, García-Ortega, L, Oñaderra, M, Gavilanes, JG and Martínez-del-Pozo, A (2007) Fungalribotoxins: molecular dissection of a family of natural killers. *FEMS Microbiol Rev* **31**: 212-237.

Lacadena, J, Mancheño, JM, Martínez-Ruiz, A, Martínez-del-Pozo, A, Gasset, M, Oñaderra, M and Gavilanes, JG (1995) Substitution of histidine-137 by glutamine abolishes the catalytic activity of the ribosome-inactivating protein α-sarcin. *Biochem J* **309**: 581-586.

Lacadena, J, Martínez-del-Pozo, A, Barbero, JL, Mancheño, JM, Gasset, M, Oñaderra, M, López-Otín, C, Ortega, S, García, JL and Gavilanes, JG (1994) Overproduction and purification of biologically active native fungal α-sarcin in *Escherichia coli*. *Gene* **142**: 147-151.

Lacadena, J, Martinez del Pozo, A, Martinez-Ruiz, A, Perez-Canadillas, JM, Bruix, M, Mancheño, JM, Onaderra, M and Gavilanes, JG (1999) Role of histidine-50, glutamic acid-96, and histidine-137 in the ribonucleolytic mechanism of the ribotoxin alpha-sarcin. *Proteins* **37**: 474-484.

Mancheño, JM, Gasset, M, Albar, JP, Lacadena, J, Martinez-del-Pozo, A, Oñaderra, M and Gavilanes, JG (1995) Membrane interaction of a β-structure-forming synthetic peptide comprising the 116-139th sequence region of the cytotoxic protein α-sarcin. *Biophys J* **68**: 2387-2395.

Mancheño, JM, Gasset, M, Lacadena, J, Ramón, F, Martínez-del-Pozo, A, Oñaderra, M and Gavilanes, JG (1994) Kinetic study of the aggregation and lipid mixing produced by α-sarcin on phosphatidylglycerol and phosphatidylserine vesicles: stopped-flow light scattering and fluorescence energy transfer measurements. *Biophys J* **67**: 1117-1125.

Mancheño, JM, Martínez-del-Pozo, A, Albar, JP, Oñaderra, M and Gavilanes, JG (1998) A peptide of nine amino acid residues from α-sarcin cytotoxin is a membrane-perturbing structure. *J Pept Res* **51**: 142-148.

Martínez-del-Pozo, A, Gasset, M, Oñaderra, M and Gavilanes, JG (1988) Conformational study of the antitumor protein α-sarcin. *Biochim Biophys Acta* **953**: 280-288.

Martínez-Ruiz, A, García-Ortega, L, Kao, R, Lacadena, J, Oñaderra, M, Mancheño, JM, Davies, J, Martínez-del-Pozo, A and Gavilanes, JG (2001) RNase U2 and α-sarcin: A study of relationships. *Methods Enzymol* **341**: 335-351.

Mazet, I and Vey, A (1995) Hirsutellin A, a toxic protein produced *in vitro* by *Hirsutella thompsonii*. *Microbiology* **141**: 1343-1348.

Olombrada, M, Herrero-Galán, E, Tello, D, Oñaderra, M, Gavilanes, JG, Martinez-del-Pozo, A and García-Ortega, L (2013) Fungal extracellular ribotoxins as insecticidal agents. *Insect Biochem Mol Biol* **43**: 39-46.

Olombrada, M, Martínez-del-Pozo, A, Medina, P, Budia, F, Gavilanes, JG and García-Ortega, L (2014a) Fungal ribotoxins: Natural protein-based weapons against insects. *Toxicon* **83**: 69-74.

Olombrada, M, Rodríguez-Mateos, M, Prieto, M, Pla, J, Remacha, M, Martínez-del-Pozo, A, Gavilanes, JG, Ballesta, JPG and García-Ortega, L (2014b) The Acidic Ribosomal Stalk Proteins Are Not Required for the Highly Specific Inactivation Exerted by α‑Sarcin of the Eukaryotic Ribosome. *Biochemistry* **53**: 1545−1547.

Oñaderra, M, Mancheño, JM, Gasset, M, Lacadena, J, Schiavo, G, Martínez-del-Pozo, A and Gavilanes, JG (1993) Translocation of α-sarcin across the lipid bilayer of asolectin vesicles. *Biochem J* **295**: 221-225.

Pérez-Cañadillas, JM, Campos-Olivas, R, Lacadena, J, Martínez-del-Pozo, A, Gavilanes, JG, Santoro, J, Rico, M and Bruix, M (1998) Characterization of pKa values and titration shifts in the cytotoxic ribonuclease α-sarcin by NMR. Relationship between electrostatic interactions, structure, and catalytic function. *Biochemistry* **37**: 15865-15876.

Pérez-Cañadillas, JM, Guenneugues, M, Campos-Olivas, R, Santoro, J, Martínez del Pozo, A, Gavilanes, JG, Rico, M and Bruix, M (2002) Backbone dynamics of the cytotoxic Ribonuclease α-sarcin by ^{15}N NMR relaxation methods. *J Biomol NMR* **24**: 301-316.

Pérez-Cañadillas, JM, Santoro, J, Campos-Olivas, R, Lacadena, J, Martínez-del-Pozo, A, Gavilanes, JG, Rico, M and Bruix, M (2000) The highly refined solution structure of the cytotoxic ribonuclease α-sarcin reveals the structural requirements for substrate recognition and ribonucleolytic activity. *J Mol Biol* **299**: 1061-1073.

Plantinga, MJ, Korennykh, AV, Piccirilli, JA and Correll, CC (2008) Electrostatic interactions guide the active site face of a structure-specific ribonuclease to its RNA substrate. *Biochemistry* **47**: 8912-8918.
Plantinga, MJ, Korennykh, AV, Piccirilli, JA and Correll, CC (2011) The ribotoxin restrictocin recognizes its RNA substrate by selective engagement of active site residues. *Biochemistry* **50**: 3004-3013.
Siemer, A, Masip, M, Carreras, N, García-Ortega, L, Oñaderra, M, Bruix, M, Martínez-del-Pozo, A and Gavilanes, JG (2004) Conserved asparagine residue 54 of α-sarcin plays a role in protein stability and enzyme activity. *Biol Chem* **385**: 1165-1170.
Tello, D, Rodríguez-Rodriguez, M, Yélamos, B, Gómez-Gutiérrez, J, Ortega, S, Pacheco, B, Peterson, DL and Gavilanes, F (2010) Expression and structural properties of a chimeric protein based on the ectodomains of E1 and E2 hepatitis C virus envelope glycoproteins. *Protein Expr Purif* **71**: 123-131.
Viegas, A, Herrero-Galán, E, Oñaderra, M, Macedo, AL and Bruix, M (2009) Solution structure of hirsutellin A. New insights into the active site and interacting interfaces of ribotoxins. *FEBS J* **276**: 2381-2390.
Wool, I (1996) Extraribosomal functions of ribosomal proteins. *Trends Biochem Sci* **21**: 164-165.
Wool, IG (1997) Structure and mechanism of action of the cytotoxic ribonuclease α-sarcin. In: *Ribonucleases* (D'Alessio, G and Riordan, JF, eds.).pp. 131-162. Academic Press, San Diego, California.
Yang, X, Gerczei, T, Glover, L and Correll, CC (2001) Crystal structures of restrictocin-inhibitor complexes with implications for RNA recognition and base flipping. *Nat Struct Biol* **8**: 968-973.
Yang, XJ and Moffat, K (1996) Insights into specificity of cleavage and mechanism of cell entry from the crystal structure of the highly specific *Aspergillus* ribotoxin, restrictocin. *Structure* **4**: 837-852.

Figures legends

Figure 1. (A) Diagrams showing the three-dimensional structure of α-sarcin (PDB ID: 1DE3) and HtA (PDB ID: 2KAA). Side chain~~s~~ of the four residues mutated in α-sarcin are shown in gray, as well as the equivalent ones equivalent in HtA, according to the sequence alignment shown in (B). α-Sarcin loop 2 backbone stretch deleted is also shown in gray. (B) Alignment of α-sarcin and HtA amino acid sequences. Residues mutated in α-sarcin are marked with an asterisk. Both the deleted residues in α-sarcin ΔSarHtA, as well as the introduced amino acids corresponding to the equivalent HtA stretch, appear underlined. Color codes: Blue for the NH_2-terminal β-hairpin and the β-strands; red for the α-helix; yellow for loop 1; green for loop 2; light blue for loop 3, magenta for loop 4; orange for loop 5. The diagrams were generated with PyMol software (DeLano 2008).

Figure 2. Far-UV circular dichroism spectra. (*Circles*) Wild-type α-sarcin, (*triangles up*) H82Q variant, and (triangles down) ΔSarHtA. *Black lines*, calculated difference spectra wild-type *minus* mutant, either H82Q or ΔSarHtA. Spectra of K111E, K112E, and K114E are not shown because they were indistinguishable from that obtained for the wild-type protein. Mean residue weight ellipticity (θ_{MRW}) is expressed in units of degree x cm^2 x $dmol^{-1}$.

Figure 3. Near-UV circular dichroism spectra. (*Circles*) Wild-type, (*triangles up*) K111E, (*triangles down*) K112E and (*squares*) K114E mutant variants of α-sarcin. Mean residue weight ellipticity (θ_{MRW}) is expressed in units of degree x cm^2 x $dmol^{-1}$.

Figure 4. Near-UV circular dichroism spectra. (*Circles*) Wild-type α-sarcin, H82Q variant (*triangles up*) and ΔSarHtA (triangles down). *Black lines*, calculated difference spectra wild-type *minus* mutant, either H82Q or ΔSarHtA. Mean residue weight ellipticity (θ_{MRW}) is expressed in units of degree x cm^2 x $dmol^{-1}$.

Figure 5. Fluorescence emission spectra of wild-type α-sarcin and the ΔSarHtA and H82Q mutants. All spectra were recorded at identical protein concentrations. Spectra labeled ‘1’ resulted from excitation at 275 nm and

spectra labeled ‘2’ from excitation at 295 nm. These spectra were normalized at wavelengths above 380 nm to obtain spectra ‘3’ (tryptophan contribution). Spectra ‘4’ (tyrosine contribution) were calculated by subtracting spectra ‘3’ from spectra ‘1’. Fluorescence emission units were arbitrary, and referred to the maximum value of wild-type α-sarcin upon excitation at 275 nm.

Figure 6. Ribonucleolytic characterization of wild-type α-sarcin and the mutant proteins studied. (A) Ribosome cleaving activity assay performed using a rabbit cell-free reticulocytes lysate. A control in the absence of enzyme is also shown (c). The highly specific ribonucleolytic activity of the ribotoxins is shown by the release of the 400-nt α-fragment (α) from the 28S rRNA of eukaryotic ribosomes. Positions of bands corresponding to 28S and 18S rRNA are also indicated. (B) Activity assay on a 35-mer oligonucleotide mimicking the SRL. A control in the absence of enzyme is also shown (c). The 21-mer and 14-mer oligonucleotides resulting from the specific cleavage of a single phosphodiester bond are indicated. The intact 35-mer oligo is also shown. (C) Zymogram assay corresponding to the non-specific ribonuclease activity of the proteins. The poly(A)-degrading activity of the proteins produces a colorless region.

Figure 7. (A) Binding of wild-type α-sarcin and the different mutants studied to DMPG vesicles. Protein bound to the vesicles (expressed as percentage) was calculated as the difference total protein minus protein remaining in the supernatant after ultracentrifugation, 100% value being the total amount of protein present. (B) DMPG vesicle aggregation induced by wild-type α-sarcin and the different mutants. Aggregation of vesicles was measured as the increase of absorbance at 360 nm, 100 seconds after the addition of the protein to a vesicle sample (ΔA_{360} nm versus protein/lipid molar ratio). (C) Leakage of intravesicular aqueous contents (relative leakage considering that produced by detergent as 100%) versus protein/lipid molar ratio. Graph symbols correspond to wild-type (black dots), H82Q (white dots), K111E (black squares), K112E (white squares), K114E (black triangles), and ΔSarHtA (white triangles).

Figure 8. Protein biosynthesis inhibition in Sf9 insect cells cultured in the presence of different concentrations of wild type α-sarcin (black dots), H82Q

(white squares), K111E (black triangles down), K112E (white triangles up), K114E (black squares), and ΔSarHtA (white dots).

Figure 9. Diagram showing the spatial distribution of Tyr 48 and 106 (yellow) and Lys 111, 112 (blue) and 114 (red) in wild-type α-sarcin (PDB ID: 1DE3). Diagram was generated using the PyMol software (DeLano 2008).

Figure 1

Click here to download high resolution image

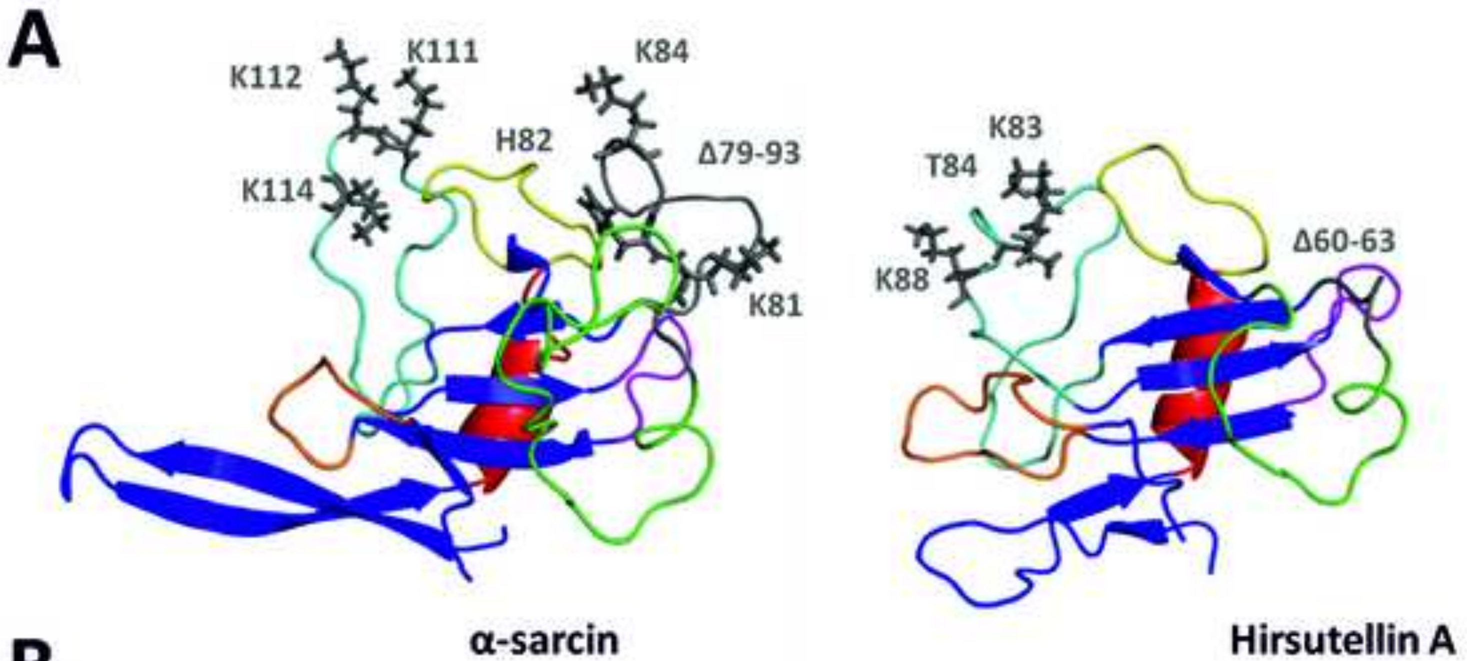

B

```
SAR : AVTWTCLNDQKNPKTNKYETKRLLYNQNKAESNSHHAPLSDGKTGSSYPHWFTN : 54
HTA : APIVTCR-----P-KLDGREKPFKVDVATAQAQARKAGLTTGKSGD--PHRYFA : 46

                                     *
SAR : GYDGDGKLPKGRTPIKFGKSDCDRPPKHSKDGNGKTDHYLLEFPTFPDGH--DY : 106
HTA : GDH-----------IRWGVNNCDK-A------D----AILWEYPIYWVGKNAEW : 78

          **   *
SAR : KFDSKK--PKENPGPARVIYTY--PNKVFCGIIAHTKE---NQGE--LKLCSH : 150
HTA : AKDVKTSQQKGGPTPIRVVYANSRGAVQYCGVMTHSKVDKNNQGKEFFEKCD- : 130
```

Figure 2

Click here to download high resolution image

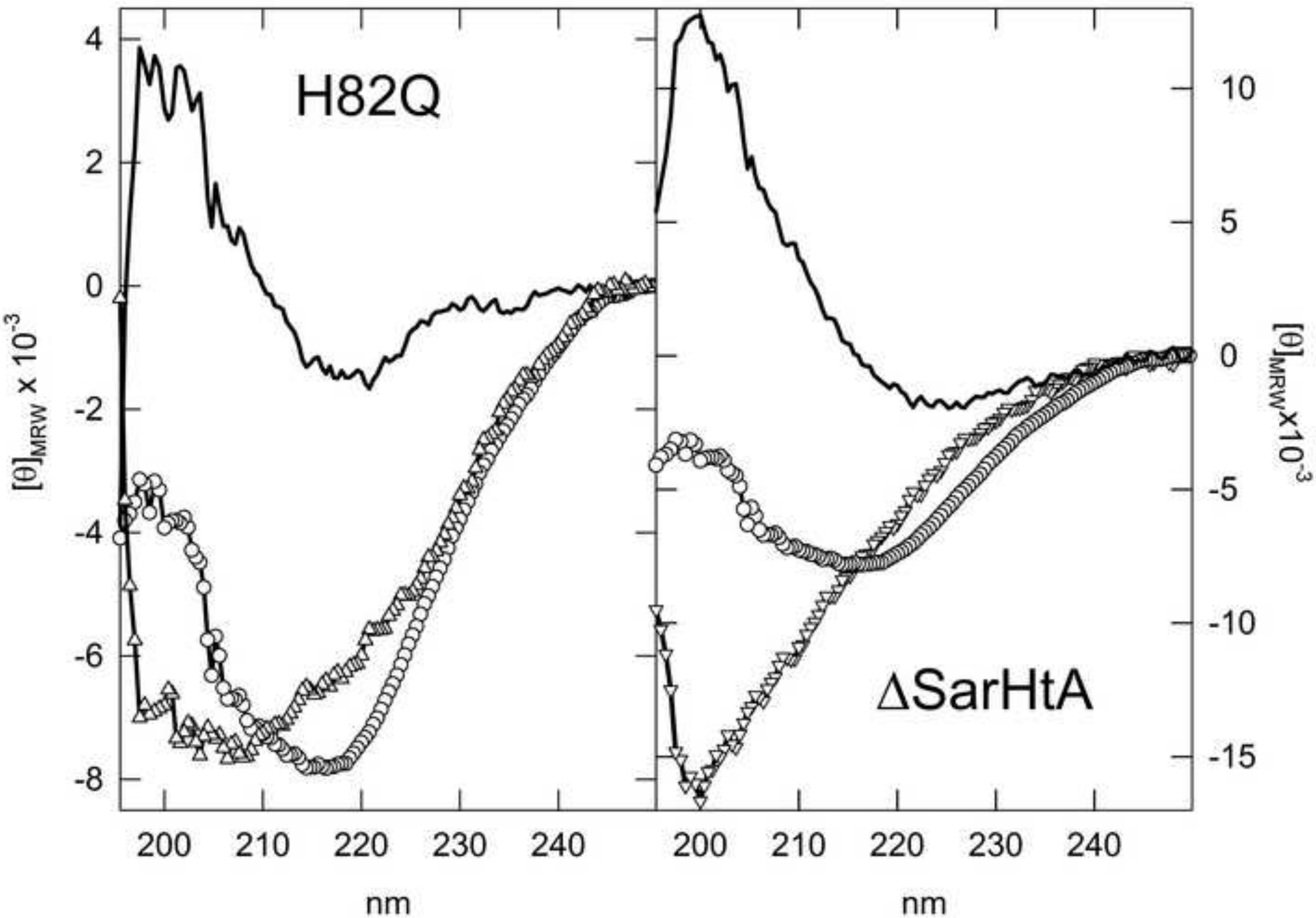

Figure 3

Click here to download high resolution image

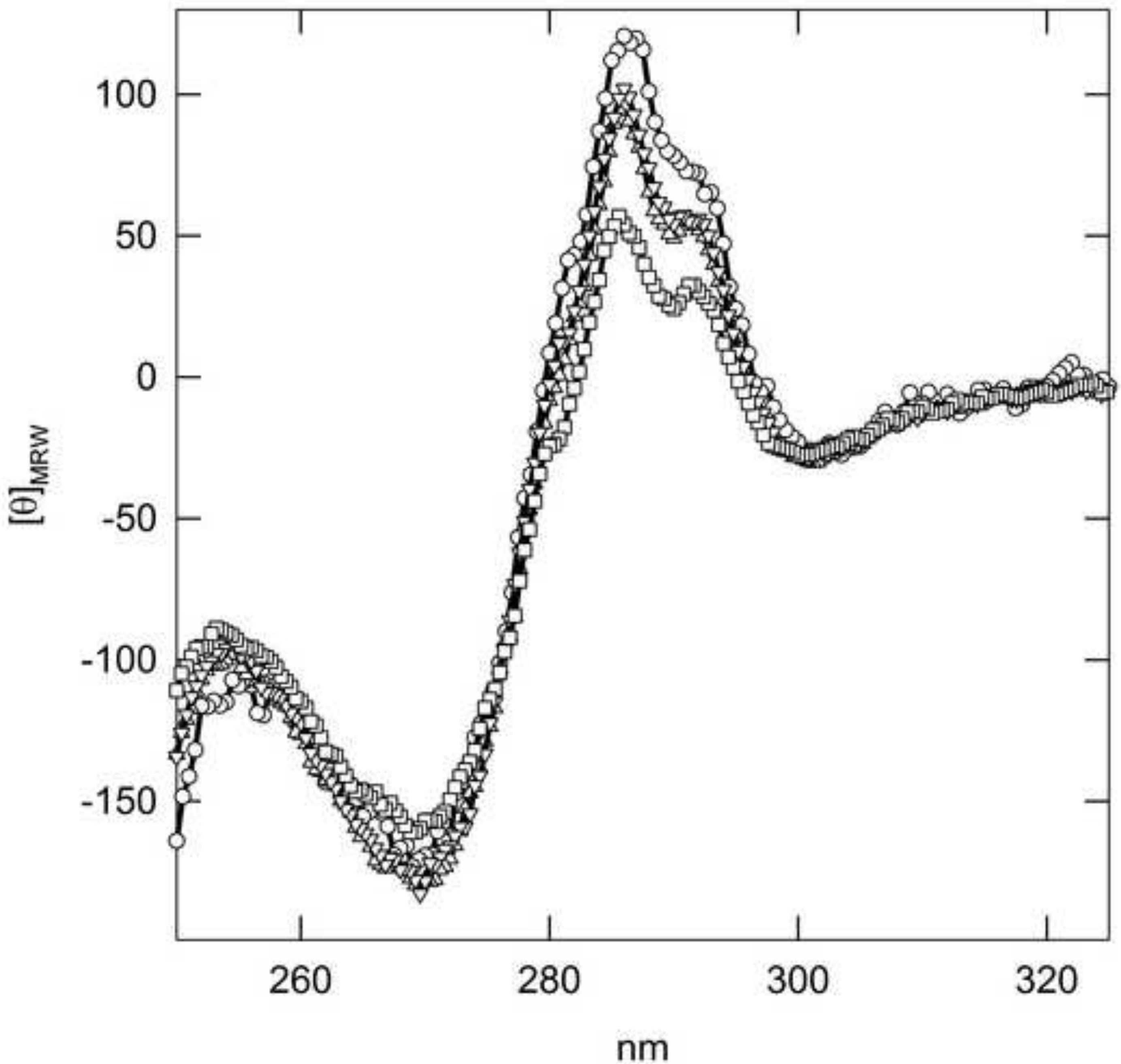

Figure 4

Click here to download high resolution image

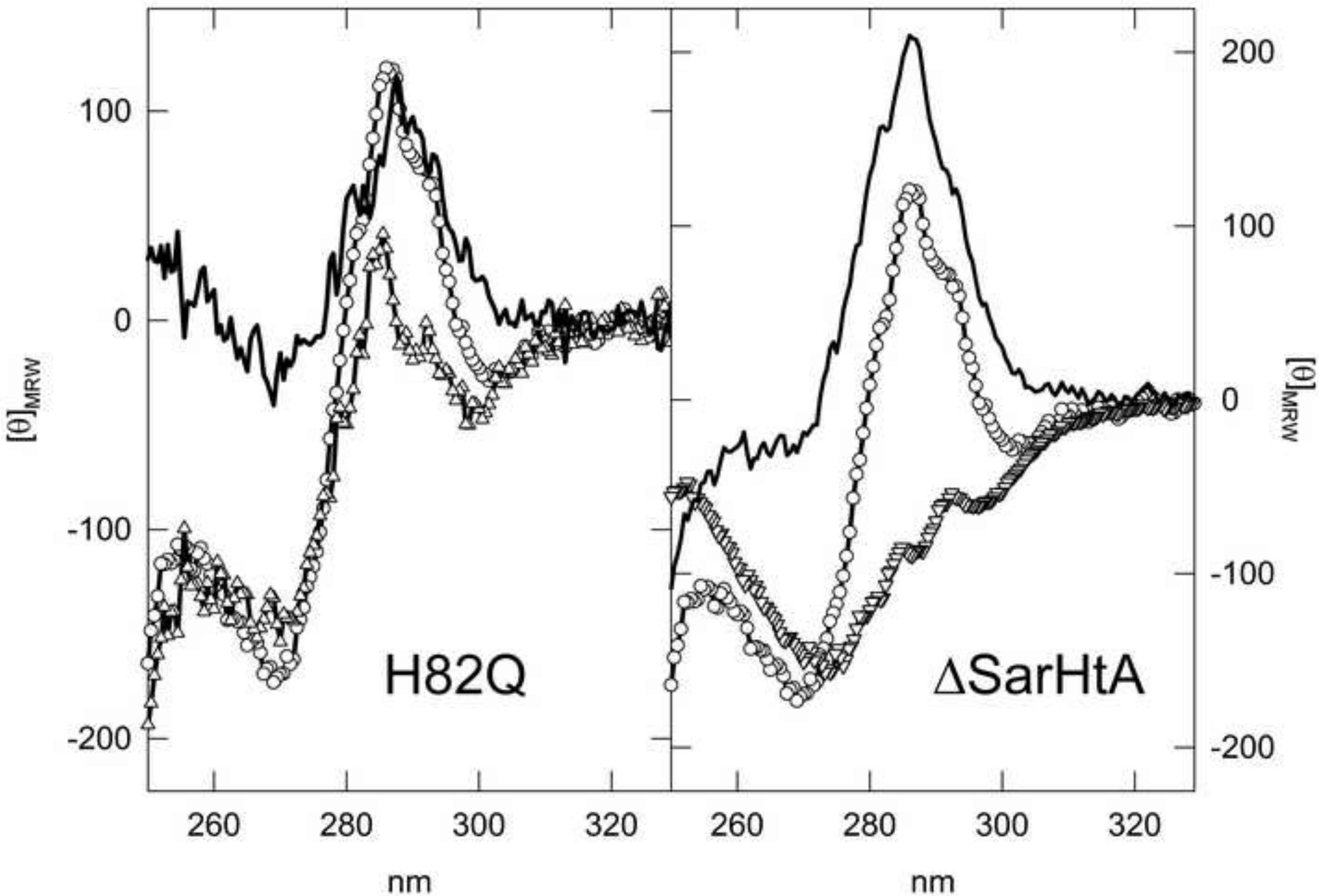

Figure 5
Click here to download high resolution image

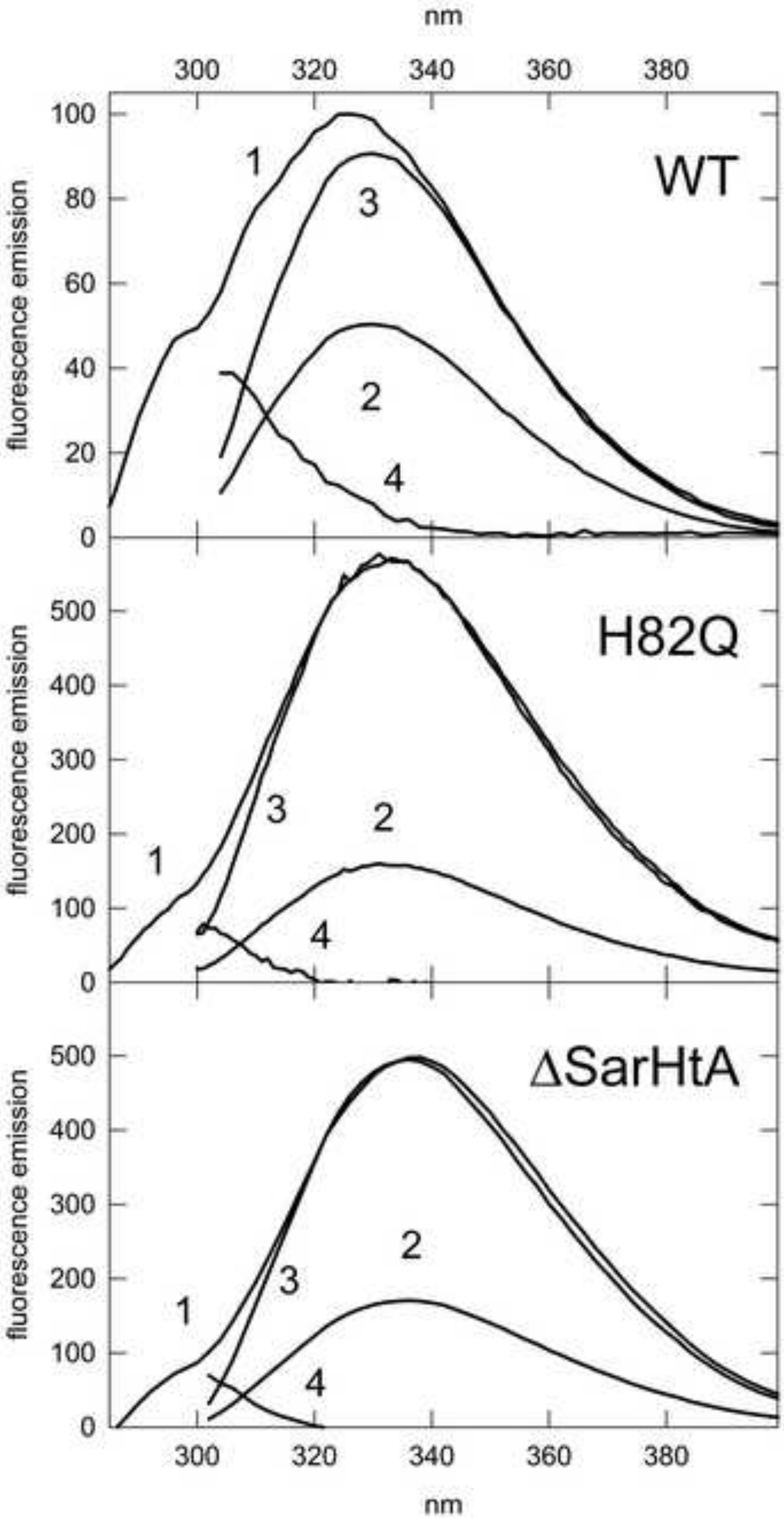

Figure 6
Click here to download high resolution image

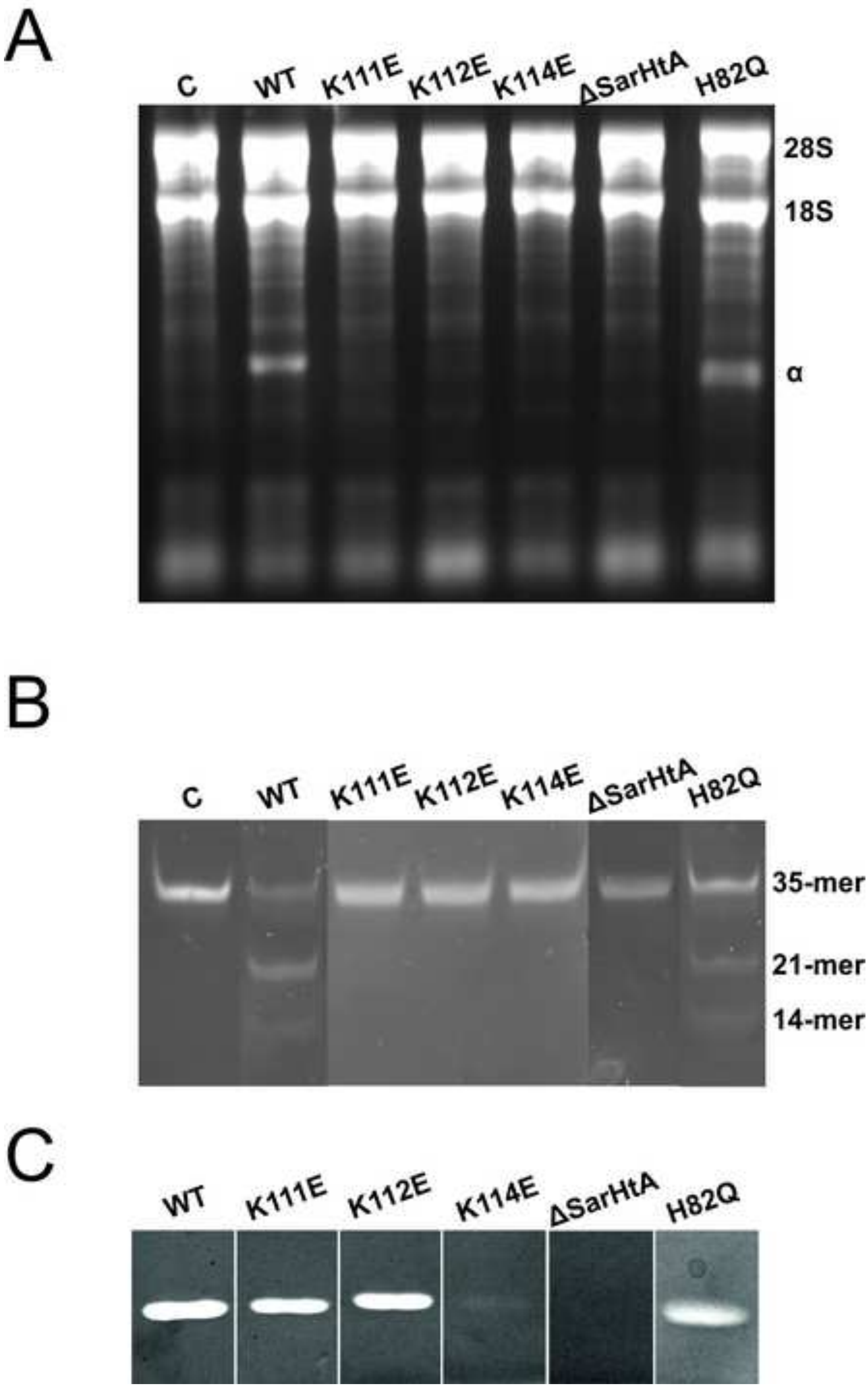

Figure 7
Click here to download high resolution image

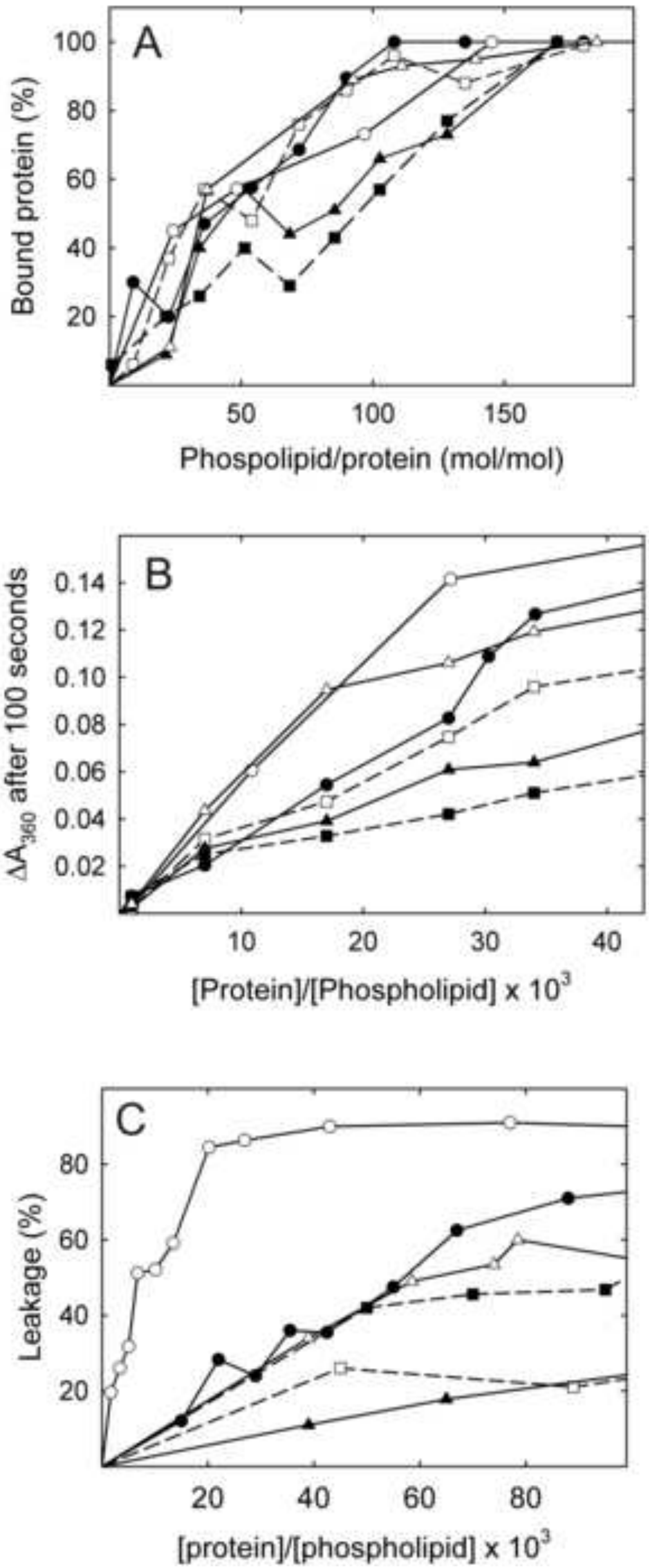

Figure
Click here to download high resolution image

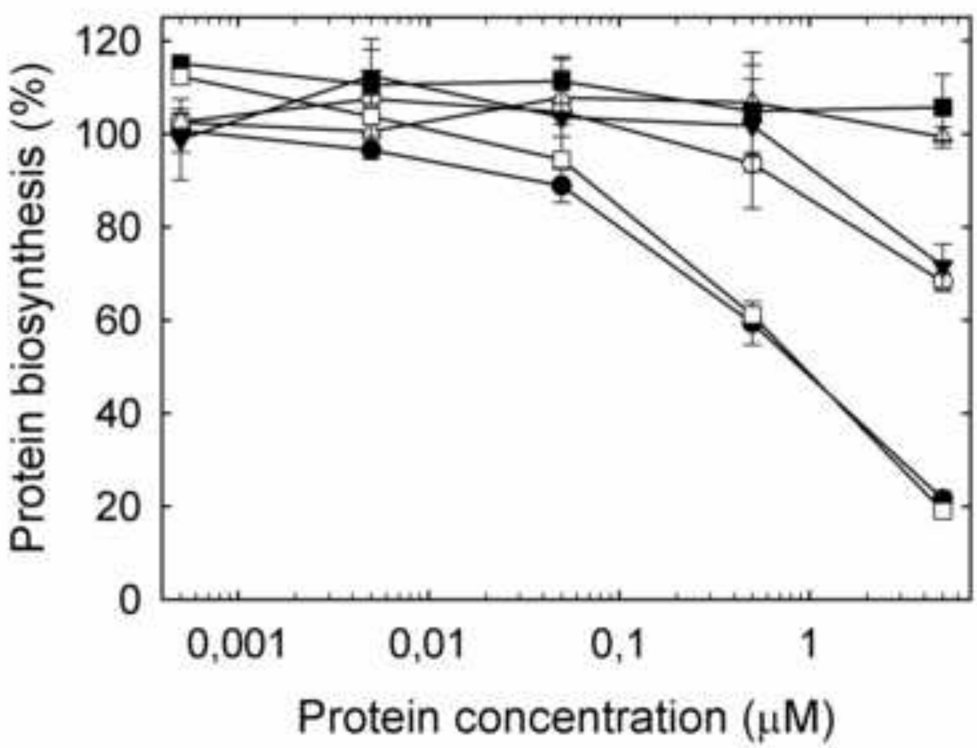

Figure 9
Click here to download high resolution image